Engineering Photon Statistics in a Spinor Polariton Condensate

S. Baryshev[1], A. Zasedatelev[1,2,*] H. Sigurdsson[3,2] I. Gnusov[1], J. D. Töpfer[2],
A. Askitopoulos,[1] and P. G. Lagoudakis[1,2]

[1]*Hybrid Photonics Laboratory, Skolkovo Institute of Science and Technology, Territory of Innovation Center Skolkovo,
Bolshoy Boulevard 30, building 1, 121205 Moscow, Russia*
[2]*School of Physics and Astronomy, University of Southampton, Southampton SO17 1BJ, United Kingdom*
[3]*Science Institute, University of Iceland, Dunhagi 3, IS-107, Reykjavik, Iceland*

We implement full polarization tomography on photon correlations in a spinor exciton-polariton condensate. Our measurements reveal condensate pseudospin mean-field dynamics spanning from stochastic switching between linear polarization components, limit cycles, and stable fixed points, and their intrinsic relation to the condensate photon statistics. We optically harness the cavity birefringence, polariton interactions, and the optical orientation of an incoherent exciton reservoir to engineer photon statistics with precise control. Our results demonstrate a smooth transition from a highly coherent to a super-thermal state of the condensate polarization components.

Photon statistics is of central importance in laser physics and quantum optics and serves as an essential toolbox for the characterization of optical sources ranging from pure single-photon to super-thermal highly fluctuating light sources. The Poissonian distribution of photon statistics in a laser defines its noise properties, whose understanding is at the heart of many applications such as laser cooling [1], precise interferometry [2], and optical communication [3]. Alongside semiconductor optical microcavities in the weak [4] and strong-coupling regime [5], particle statistics of heavily correlated many-body systems such as atomic [6] and photonic Bose-Einstein condensates [7] retain strong interest.

While an ideal laser obeys a Poissonian photon distribution, practical devices usually suffer from excessive noise that broadens the distribution, affecting phase stability. Mode competition is one detrimental effect generating excessive, so-called, super-Poisson noise in conventional semiconductor microcavity lasers [8–10]. At the same time, stochastic mode switching allows for studying intriguing phenomena of chaos in photonic systems [11] and opens the door for new optoelectronic applications such as ghost imaging [12] and multiphoton microscopy [13] with superbunched light, while mode beating enables low-energy ultrafast optical communications [14]. The intrinsic linear mode coupling usually dominates over nonlinear effects in conventional microlasers. However, in semiconductor structures with strong light-matter interactions, nonlinear effects can dominate mode coupling.

Exciton polaritons (from here on polaritons) are bosonic quasiparticles originating from strong light-matter coupling of excitons with photons in semiconductor microcavities [15]. They can undergo nonequilibrium Bose-Einstein condensation [16] into a spinor order parameter $\Psi = (\psi_+, \psi_-)^T$ corresponding to the right-hand σ^+ and left-hand σ^- circular polarization of the emitted light like in a conventional semiconductor spin laser [17]. Besides its fundamental importance, the spin degree of freedom is particularly attractive for applications [18]. The exciton component makes the polariton Bose gas inherently non-linear due to pair-particle interactions, permitting experimental observation of quantum correlations [19,20] and superfluidity [21,22]. Particle number fluctuations and statistics are intimately connected to the linewidth of polariton condensates, playing an essential role in understanding the fundamental limits of their coherence properties [23]. Today, polariton condensates offer unprecedented all-optical control for building large interacting nonlinear networks [24] and devices ranging from amplifiers [25,26], transistors [27–29], tunneling diodes [30], routers [31–33], phase-controlled interferometers [34], topological insulators [35], and switches [36–38] to volatile memory elements [39]. The coherence time of polariton condensates under resonant excitation was shown to reach up to ~ns in the optical-parametric-oscillation regime [40]. However, under nonresonant excitation and in the presence of an incoherent exciton reservoir, the coherence time is limited to ~10–100 ps [41–45]. Furthermore, the presence of an exciton reservoir causes depolarization [46], which was evidenced through spinor dephasing in second-order photon correlation measurements [47].

In this Letter, we demonstrate engineering of photon statistics in a spinor polariton condensate utilizing an optical trap configuration to separate the condensate from the exciton reservoir, extending its coherence time over 2 orders of magnitude, from ~50 ps to ~1 ns [48,49].

We note, here, that the polariton lifetime is $\tau_p = 6.5$ ps. Long coherence times, in combination with steady-state (continuous-wave) optical pumping, allow for the study of the spinor dynamics in the absence of the condensate density transients that dominate the dynamics under short-pulsed optical excitation [47]. By applying polarization resolved photon correlation measurement on all three Stokes components, we observe regimes of stochastic switching between linear polarization components of the condensate emission, as well as limit cycles and stable fixed points of its spinor. We tune the excitation parameters demonstrating a crossover from superthermal photon distribution to a highly coherent state.

The condensate is created in GaAs-AlAs$_{0.98}$P$_{0.02}$ 2λ microcavity with embedded InGaAs quantum wells [50] held in a cryostat at 4K with exciton-cavity detuning of -3 meV. We excite our sample nonresonantly at the first Bragg minimum of the reflectivity stop band, $\lambda_{\text{ext}} = 783$ nm, with a linearly polarized laser. The beam is acousto-optically modulated with a square waveform at 1 kHz frequency and 10% duty cycle, and its profile is shaped into an annular optical trap with 12 μm diameter as shown in Fig. 1(a). As the condensate forms in the center of the optical trap, its overlap with the photoexcited reservoir of uncondensed excitons is minimized; see bottom panel of Fig. 1(a). We extract statistical information of the Stokes parameters $\mathbf{S} = (S_1, S_2, S_3)$, which correspond to horizontal-vertical (S_1), diagonal-antidiagonal (S_2), and right- and

left-hand circular (S_3) polarization of the emitted cavity light as presented in Fig. 1(b). Orthogonal polarization components are mapped on the different pseudospin projections of the polariton condensate and defined as

$$\mathbf{S} = \frac{1}{2}\Psi^\dagger \boldsymbol{\sigma} \Psi, \tag{1}$$

with $\boldsymbol{\sigma}$ being the Pauli matrix vector. A polarization resolving Hanbury-Brown-Twiss (HBT) intensity interferometer ($\mathcal{I}_i$) enables direct measurement of second-order photon auto- and cross-correlation functions

$$g_{i,j}^{(2)}(\tau) = \frac{\langle a_i^\dagger(t) a_j^\dagger(t+\tau) a_j(t+\tau) a_i(t)\rangle}{\langle a_i^\dagger(t) a_i(t)\rangle \langle a_j^\dagger(t+\tau) a_j(t+\tau)\rangle}, \tag{2}$$

where $a_i^\dagger$ and a_i are photon creation and annihilation operators for given polarizations i, j denoted horizontal (H), vertical (V); diagonal (D), antidiagonal (AD); and left-circular (LC), right-circular (RC) polarizations, and τ is the time-delay between photon detection events. The angled brackets $\langle . \rangle$ indicate time average over millions of condensate realizations (i.e., the system is ergodic). In the following, we implement a polarization-resolving multichannel HBT intensity interferometer to measure second order auto- and cross-correlations between the pseudospin projections as schematically illustrated in Fig. 1(c).

Figure 2(a) shows the second-order correlation function in the absence of polarization filtering, at the condensation threshold ($P = P_{\text{th}}$), and above threshold ($P = 1.31 P_{\text{th}}$) for horizontally polarized excitation. We observe a small photon bunching $g^{(2)}(0) \approx 1.04$ at threshold with $\tau_c = 220$ ps second-order correlation time derived from a Gaussian fit to the data. Increasing the excitation density above condensation threshold drives the condensate toward a highly coherent state as evidenced by the disappearance of photon bunching on top of the shot noise level, $g^{(2)}(0) \simeq 1$, in agreement with previous studies [23,45,51]. We did not observe any measurable deviation from the coherent state with increasing pump power up to $3.5 P_{\text{th}}$.

Further on, we use polarization filtering to detect the photon statistic of the Stokes parameters. For pumping levels above condensation threshold, wherein the polariton condensate is highly coherent, $1.31 P_{\text{th}}$, the polarization filtered photon statistics on the circular components, S_3, for both co-, and cross-circular detection, is Poissonian as shown in Fig. 2(b). However, the $S_{1,2}$ projections obey super-Poissonian photon distribution, $g_{i,i}^{(2)}(0) > 1$, as shown for different linear polarization components in Figs. 2(c) and 2(d). This excess noise is attributed to a random orientation of the condensate pseudospin in the equatorial plane of the Poincaré sphere due to spontaneous breaking of the $U(1)$ symmetry [42,52,53] from realization to realization. Moreover, with no additional mechanism
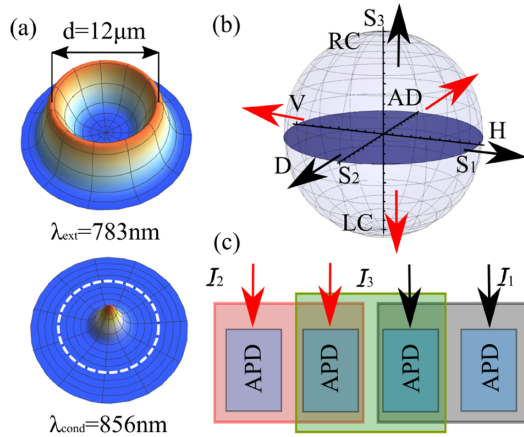

FIG. 1. (a) Schematic presentation of the annular optical trap (upper panel) and condensate emission (lower panel). White dashed line outlines the optical trap. (b) Poincaré sphere showing three sets of the condensate pseudospin projections onto Stokes parameters. (c) HBT interferometers $\mathcal{I}_1$ (black box) and $\mathcal{I}_2$ (red box) are dedicated to measure intensity autocorrelation for orthogonal pseudospin projections indicated by black and red arrows, respectively [e.g., $\mathcal{I}_1$ measures $g_{\text{H,H}}^{(2)}(\tau)$ and $\mathcal{I}_2$ measures $g_{\text{V,V}}^{(2)}(\tau)$]. At the same time $\mathcal{I}_3$ (green box) measures cross-correlation between these projections [i.e., $g_{\text{H,V}}^{(2)}(\tau)$]. APD refers to Avalanche photo diode.
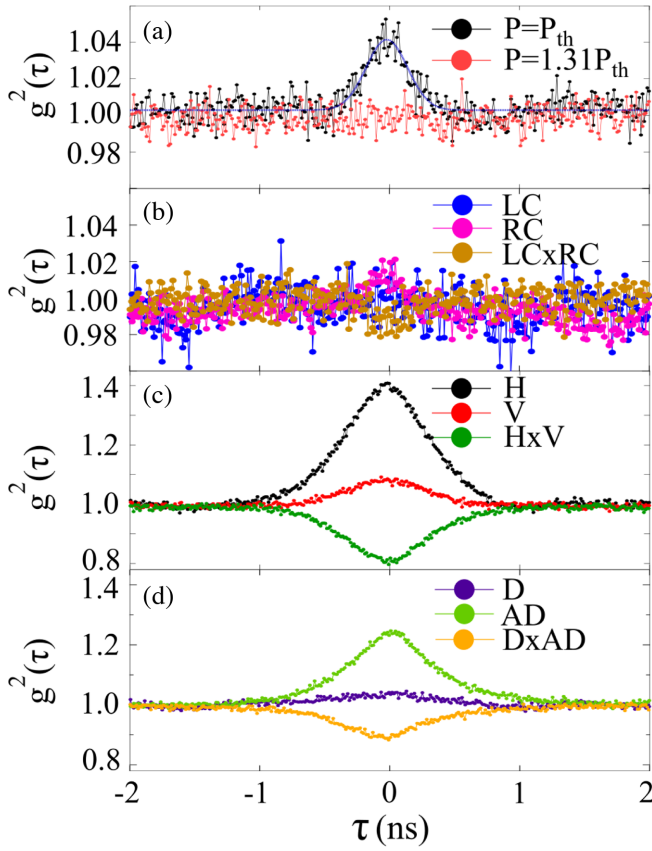
FIG. 2. (a) Second order correlation function of the condensate, measured without polarization filtering at $P = P_{th}$ and $P = 1.31P_{th}$. Blue line is a Gaussian fit. (b)–(d) $g_{i,i}^{(2)}(\tau)$, $g_{j,j}^{(2)}(\tau)$, and $g_{i,j}^{(2)}(\tau)$ at $P = 1.31P_{th}$ for LC-RC, H-V, and D-AD polarizations, respectively (letter "x" denoting cross correlation).

distinguishing between different linear polarizations of the pseudospin, one can intuitively expect it walking randomly in the equatorial plane due to polariton-polariton interactions [54], which would lead to equal bunching amplitudes for all linear polarizations.

The observation of unequal bunching between the linear polarization components is attributed to structural disorder induced birefringence in the microcavity, which breaks the planar symmetry [55]. This leads to a linear polarization energy splitting analogous to an in-plane effective magnetic field, $\Omega_\parallel(\mathbf{r}) = (\Omega_x, \Omega_y)^T$, that varies randomly across the sample. It was theoretically predicted that polariton-polariton interactions align (pin) the condensate pseudospin parallel to the field [56–58], which leads to the unequal bunching between the different linear polarizations, $S_{1,2}$ observed in Figs. 2(c) and 2(d).

Analysis of photon cross correlations in this pinned regime gives important insight into the complex dynamics of the pseudospin. Panels (c) and (d) in Fig. 2 reveal anticorrelated photon fluctuations between orthogonal projections. This means that fluctuations in one projection

inevitably induce fluctuations in the orthogonal one. Namely, the anticorrelated behavior $g_{i,j}^{(2)}(0) < 1$ corresponds to temporal switching of the pseudospin direction in the equatorial plane from being parallel to antiparallel with $\Omega_\parallel(\mathbf{r})$. Such switching events can be understood as mode competition between two fixed point attractors in the pseudospin phase space, with the pinned $\mathbf{S}\parallel\Omega_\parallel$ attractor being much stronger than the antiparallel $-\mathbf{S}\parallel\Omega_\parallel$ attractor [59]. In Section I in the Supplemental Material (SM [60]), we show that the switching between parallel and antiparallel alignment of the pseudospin occurs randomly in time. The switching strongly affects the photon statistics of the linearly polarized projections, especially those which are antiparallel to the pinning field. Indeed, we observe the highest value of $g_{i,i}^{(2)}(0)$ in Figs. 2(c) and 2(d) for horizontal and antidiagonal projections. For the chosen sample location, corresponding to the data in Fig. 2, $\Omega_\parallel(\mathbf{r})$ causes the pseudospin to become pinned between the diagonal and vertical projections (See Sec. I in the SM [60] for data at a different point on the sample).

Our experiments show a significant effect of nonlinear dynamics on the photon statistics which can be controlled through the power of the optical excitation. We note that the photon autocorrelation $g_{i,i}^{(2)}(0)$ at zero time delay relates directly to the variance σ_i^2 and mean value $\bar{n}_i$ of the photon distribution according to

$$g_{i,i}^{(2)}(0) = 1 + \frac{\sigma_i^2 - \bar{n}_i}{\bar{n}_i^2}. \tag{3}$$

Figure 3(a) shows that, with increasing pump power, we observe an increase of $g_{H,H}^{(2)}(0)$ (black circles) that corresponds to photon distribution broadening (not shown). While the horizontal component experiences very strong photon number fluctuations with $g_{H,H}^{(2)}(0) \approx 1.9$ at $P \approx 1.5P_{th}$, approximating the statistics of thermal light, $g^{(2)}(0) = 2$, the vertical component is in a highly coherent state, $g_{V,V}^{(2)}(0) \approx 1.02$, as shown by the red circles of Fig. 3(a). This dependence originates from the large difference in populations between H and V projections and the stochastic switching of the pseudospin, as schematically shown in Fig. 3(b). The interdependence of the H and V projections is evidenced by their cross-correlation measurement, $g_{H,V}^{(2)}(0)$, which exhibits an anticorrelation with the V projection, as shown by the green circles of Fig. 3(a).

Evolution of the pseudospin and correspondent intensity fluctuations are qualitatively reproduced by a stochastic generalized Gross-Pitaevskii mean-field model in the truncated Wigner approximation [56,69] (for details see Sec. II in the SM [60]) as shown with solid lines in Fig. 3(a). Note that, near the condensation threshold, where
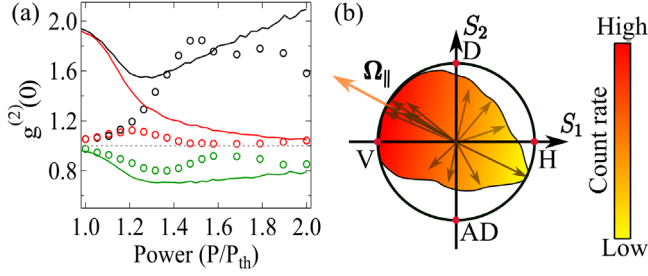
FIG. 3. (a) Measured (circles) and theoretical (solid lines) $g_{H,H}^{(2)}(0)$ (black), $g_{V,V}^{(2)}(0)$ (red), and $g_{H,V}^{(2)}(0)$ (green) power dependencies for linearly polarized excitation. Error bars for the experimental data are smaller than the size of the circled markers. (b) Schematic representation of the in-plane magnetic field (orange arrow denoted as $\mathbf{\Omega}_{\parallel}$) and the polarization of different photon occurrences (black transparent arrows). When pinned, the pseudospin is dominantly orientated parallel $\mathbf{\Omega}_{\parallel}$ (indicated by big number of co-oriented arrows) whereas random switching events change the pseudospin to antiparallel direction (indicated as few antiparallel arrows), corresponding to anticorrelated event between linear polarization components. Color scale represents total correlation photon count rate.

FIG. 4. Photon statistics engineering with excitation ellipticity. $g_{H,H}^{(2)}(\tau)$ at pump power $P = 3.5P_{\text{th}}$ for a range of ellipticities ϵ. Data for $\epsilon = 0$ and 0.007 are fitted by an exponential function (red line) $g_{H,H}^{(2)}(\tau) = 1 + [g_{H,H}^{(2)}(0) - 1]e^{-2|\tau|/\tau_c}$, data for higher ellipticity are fitted with a product of a Gaussian function and a cosine function $g_{H,H}^{(2)}(\tau) = 1 + \cos(\omega\tau)[g_{H,H}^{(2)}(0) - 1]e^{-\pi(\tau/\tau_c)^2}$ where τ_c is correlation (i.e., dephasing) time.

time resolution severely limits correlation measurements, such standard mean-field theories fail to describe high-order correlations [70,71]. At higher powers, the calculated $g_{H,H}^{(2)}(0)$ exceeds the experimental values due to the monotonic increase of the vertically polarized condensate population. This overestimation in modeling can be countered by including small polarization ellipticity in the beam as detailed in Sec. III in the SM [60].

Next, we investigate how the pseudospin dynamics under elliptically polarized pumping affect the photon statistics. In this case, the exciton reservoir which provides gain to the condensate becomes spin imbalanced (optically oriented) and follows the laser circular polarization to some degree. The stimulated nature of polariton scattering into the condensate preserves the exciton spin resulting in a condensate cocircularly polarized with the laser [72,73]. Because of strong anisotropic particle interactions, such spin population imbalance in both the condensate and the reservoir results in a nonlinear effective out-of-plane magnetic field $\mathbf{\Omega}_{\perp} = \Omega_z\hat{\mathbf{z}}$ that gives rise to self-induced Larmor precession [54,74–78] driving self-sustained periodic orbitals in the dynamical equations of motion. This field can be written as $\Omega_z \propto \alpha S_3 + g(X_+ - X_-)$, where α denotes the polariton-polariton interaction strength, g the polariton-exciton interaction strength, and $X_{\pm}$ are the exciton reservoir spin populations. The sign and the magnitude of Ω_z can be controlled through the ellipticity ϵ of the pump laser [58,79].

Figure 4 shows $g_{H,H}^{(2)}(\tau)$ at $P = 3.5P_{\text{th}}$ for excitation polarization ellipticity varying from 0 (top) to 0.361 (bottom). Under linearly polarized excitation ($\epsilon = 0$)
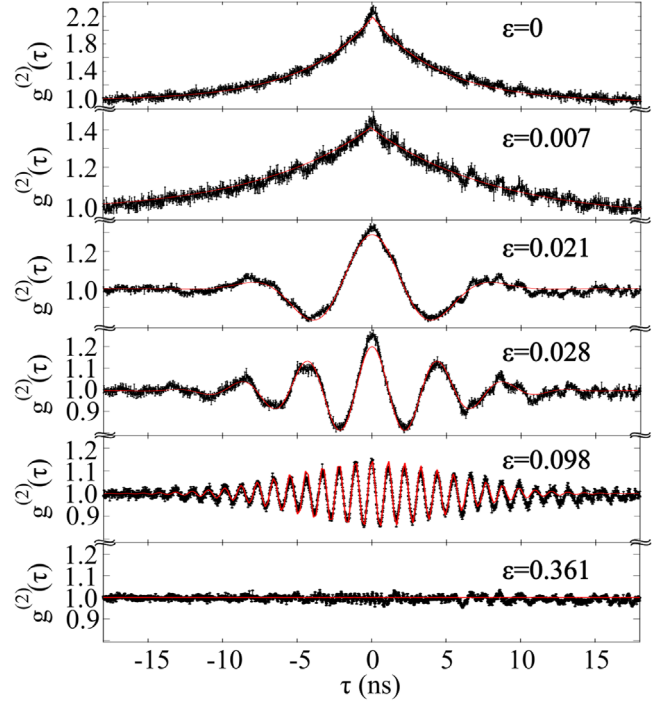
horizontal pseudospin projection gives $g_{H,H}^{(2)}(0) \approx 2.4$ with correlation time $\tau_c = 9.2$ ns. We point out that the data presented in Fig. 4 were obtained at a different sample location than those in Figs. 2 and 3, which results in quantitative differences due to different strengths and direction of the effective fields $\mathbf{\Omega}_{\parallel}(\mathbf{r}_1) \neq \mathbf{\Omega}_{\parallel}(\mathbf{r}_2)$. For ellipticities $\epsilon \geqslant 0.021$, we observe an oscillatory behavior in the photon correlations, evidencing the self-sustained Larmor precession of the pseudospin due to the combined effects of the nonlinear field $\mathbf{\Omega}_{\perp}$ and the linear birefringent field $\mathbf{\Omega}_{\parallel}$. The Larmor precession drives harmonic photon number oscillations between the orthogonal components in antiphase, which is evidenced by the photon cross correlations $g_{H,V}^{(2)}$ in the bottom panel of Fig. 5(a). To illustrate these dynamics, we simulated the condensate pseudospin trajectories for the case of $\epsilon = 0.028$. Figure 5(b) shows the trajectory of the pseudospin on the Poincaré sphere and its projection on the equatorial plane. Assuming that the in-plane birefringent field is weak compared to the out-of-plane field (i.e., $|\mathbf{\Omega}_{\perp}| > |\mathbf{\Omega}_{\parallel}|$), the precession frequency of the pseudospin is approximately dictated by the population imbalance of excitons and polaritons [78]. In Fig. 5(c), we plot the oscillation frequency from $g_{H,H}^{(2)}(\tau)$ and the
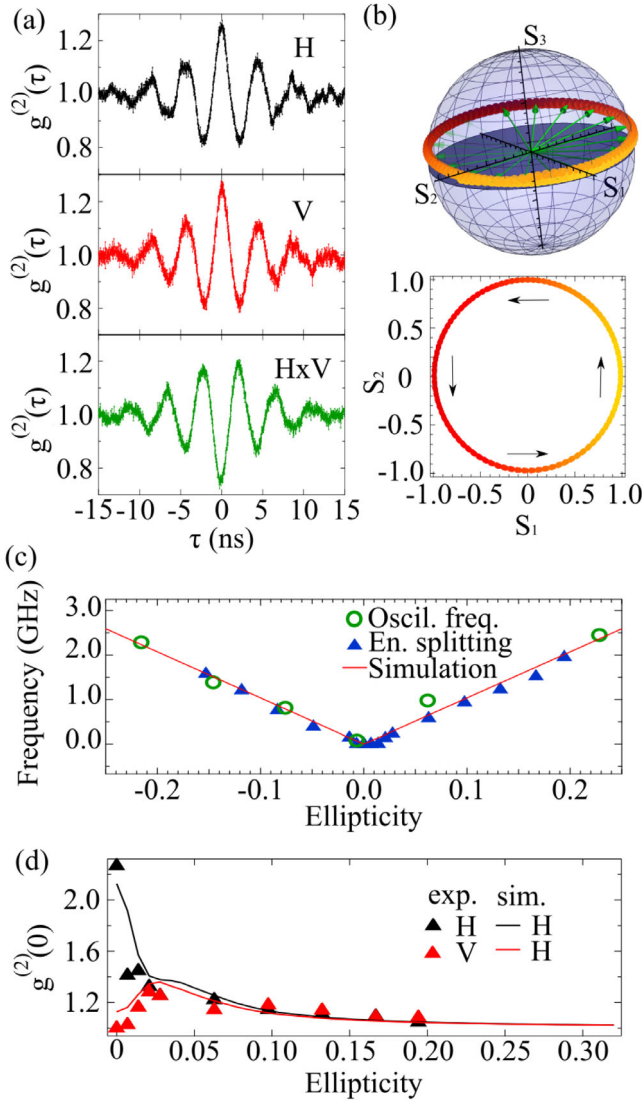
FIG. 5. (a) $g_{H,H}^{(2)}(\tau)$ (black), $g_{V,V}^{(2)}(\tau)$ (red), and $g_{H,V}^{(2)}(\tau)$ (green) at $P = 3.5P_{th}$, $\epsilon = 0.028$. (b) Calculated normalized pseudospin precession trajectory and its projection into equatorial plane of the Poincaré sphere. (c) Oscillation frequency of $g_{i,j}^{(2)}(\tau)$ (blue triangles) plotted alongside with energy splitting (green circles) between LC and RC polarized condensate. Solid red line represents simulated results. (d) Experimental (triangles) and simulated (solid line) $g_{H,H}^{(2)}(0)$ (black) and $g_{V,V}^{(2)}(0)$ (red) for different pump ellipticities.

experimentally measured energy splitting between the two counter-circular polarization components. Our numerical simulations of the splitting show excellent agreement with the experiment.

While the frequency of the $g_{H,H}^{(2)}(\tau)$ oscillations is increasing linearly with the pump ellipticity, their amplitude drops to zero at high ellipticity as the pseudospin becomes predominantly aligned toward circular projections (i.e., $|\mathbf{S}| \approx |S_3|$) converging to a stable fixed point solution close to the poles of the Poincaré sphere. Thus, the effective

out-of-plane magnetic field $\mathbf{\Omega}_\perp$ mitigates the role of the in-plane effective field $\mathbf{\Omega}_\parallel$ leading to the suppression of photon noise in the horizontal projection. Figure 4 demonstrates the effect of gradual decrease in $g_{H,H}^{(2)}(0)$ with increasing ellipticity. In Fig. 5(d), we plot $g_{H,H}^{(2)}(0)$ and $g_{V,V}^{(2)}(0)$ and observe that the photon bunching is approaching unity with increasing ellipticity. Therefore, a delicate control over the exciton and polariton spin imbalance offers a full range of tunability in photon statistics spanning from superthermal at $\epsilon \sim 0$ to super-Poissionian distributions and highly coherent states at large $\epsilon > 0.2$. We note that, in the presence of a finite $|\mathbf{\Omega}_\parallel|$, we always observe the reported behavior of the correlation functions.

In conclusion, we have realized multidimensional photon correlation tomography of an optically trapped spinor polariton condensate across its full polarization basis. Our findings demonstrate an extremely long spinor dephasing time of $\tau_c = 9.2$ ns and the unique nonlinear mean field dynamics of the condensate pseudospin on the photon statistics with tunable crossover from superthermal photon distribution to a coherent state. Such long dephasing time, $\sim 10^3$ more than the polariton lifetime, allows the observed photon statistics to become influenced by the nonlinear dynamical timescales of the coherent (mean-field) condensate. We identify stochastic linear polarization switching due to the inherent cavity birefringence resulting in polarization sensitive photon bunching and self-induced Larmor precessions in the GHz frequency range visible as oscillations in the linear polarized photon $g_{i,j}^{(2)}(\tau)$ persistent for more than 10 ns. Our findings allow for the evaluation of the noise characteristics of spin-polarized polariton lasers as well as pave the way toward exploiting nonlinear mean-field dynamics of strongly nonequilibrium bosonic systems to fine control their photon statistics.

The data that support the findings of this study are openly available from the University of Southampton repository [80].

*A.Zasedatelev@skoltech.ru

[1] A. H. Safavi-Naeini, J. Chan, J. T. Hill, S. Gröblacher, H. Miao, Y. Chen, M. Aspelmeyer, and O. Painter, Laser noise in cavity-optomechanical cooling and thermometry, New J. Phys. **15**, 035007 (2013).

[2] C. M. Caves, Quantum-mechanical noise in an interferometer, Phys. Rev. D **23**, 1693 (1981).

[3] K. Banaszek, L. Kunz, M. Jachura, and M. Jarzyna, Quantum limits in optical communications, J. Lightwave Technol. **38**, 2741 (2020).

[4] J. Wiersig, C. Gies, F. Jahnke, M. Aßmann, T. Berstermann, M. Bayer, C. Kistner, S. Reitzenstein, C. Schneider, S. Höfling, A. Forchel, C. Kruse, J. Kalden, and D. Hommel, Direct observation of correlations between individual photon emission events of a microcavity laser, Nature (London) **460**, 245 (2009).

[5] M. Aßmann, J.-S. Tempel, F. Veit, M. Bayer, A. Rahimi-Iman, A. Löffler, S. Höfling, S. Reitzenstein, L. Worschech, and A. Forchel, From polariton condensates to highly photonic quantum degenerate states of bosonic matter, Proc. Natl. Acad. Sci. U.S.A. **108**, 1804 (2011).

[6] A. Perrin, R. Bücker, S. Manz, T. Betz, C. Koller, T. Plisson, T. Schumm, and J. Schmiedmayer, Hanbury Brown and Twiss correlations across the Bose-Einstein condensation threshold, Nat. Phys. **8**, 195 (2012).

[7] B. T. Walker, J. D. Rodrigues, H. S. Dhar, R. F. Oulton, F. Mintert, and R. A. Nyman, Non-stationary statistics and formation jitter in transient photon condensation, Nat. Commun. **11**, 1390 (2020).

[8] M. B. Willemsen, M. P. van Exter, and J. P. Woerdman, Anatomy of a Polarization Switch of a Vertical-Cavity Semiconductor Laser, Phys. Rev. Lett. **84**, 4337 (2000).

[9] H. A. M. Leymann, C. Hopfmann, F. Albert, A. Foerster, M. Khanbekyan, C. Schneider, S. Höfling, A. Forchel, M. Kamp, J. Wiersig, and S. Reitzenstein, Intensity fluctuations in bimodal micropillar lasers enhanced by quantum-dot gain competition, Phys. Rev. A **87**, 053819 (2013).

[10] C. Redlich, B. Lingnau, S. Holzinger, E. Schlottmann, S. Kreinberg, C. Schneider, M. Kamp, S. Höfling, J. Wolters, S. Reitzenstein, and K. Lüdge, Mode-switching induced super-thermal bunching in quantum-dot microlasers, New J. Phys. **18**, 063011 (2016).

[11] F. Albert, C. Hopfmann, S. Reitzenstein, C. Schneider, S. Höfling, M. Kamp, W. Kinzel, A. Forchel, and I. Kanter, Observing chaos for quantum-dot microlasers with external feedback, Nat. Commun. **2**, 366 (2011).

[12] P. Ryczkowski, M. Barbier, A. T. Friberg, J. M. Dudley, and G. Genty, Ghost imaging in the time domain, Nat. Photonics **10**, 167 (2016).

[13] A. Jechow, M. Seefeldt, H. Kurzke, A. Heuer, and R. Menzel, Enhanced two-photon excited fluorescence from imaging agents using true thermal light, Nat. Photonics **7**, 973 (2013).

[14] M. Lindemann, G. Xu, T. Pusch, R. Michalzik, M. Hofmann, I. Žutić, and N. Gerhardt, Ultrafast spin-lasers, Nature (London) **568**, 212 (2019).

[15] C. Weisbuch, M. Nishioka, A. Ishikawa, and Y. Arakawa, Observation of the Coupled Exciton-Photon Mode Splitting in a Semiconductor Quantum Microcavity, Phys. Rev. Lett. **69**, 3314 (1992).

[16] J. Kasprzak, M. Richard, S. Kundermann, A. Baas, P. Jeambrun, J. Keeling, F. M. Marchetti, M. Szymańska, R. André, J. Staehli, V. Savona, P. Littlewood, B. Deveaud, and D. Le Si, Bose–Einstein condensation of exciton polaritons, Nature (London) **443**, 409 (2006).

[17] N. C. Gerhardt and M. R. Hofmann, Spin-controlled vertical-cavity surface-emitting lasers, Adv. Opt. Technol. **2012**, 268949 (2012).

[18] T. Liew, I. Shelykh, and G. Malpuech, Polaritonic devices, Physica (Amsterdam) **43E**, 1543 (2011).

[19] A. Delteil, T. Fink, A. Schade, S. Höfling, C. Schneider, and A. İmamoğlu, Towards polariton blockade of confined exciton–polaritons, Nat. Mater. **18**, 219 (2019).

[20] G. Muñoz-Matutano, A. Wood, M. Johnsson, X. Vidal, B. Baragiola, A. Reinhard, A. Lemaître, J. Bloch, A. Amo, G. Nogues, B. Besga, M. Richard, and T. Volz, Emergence of quantum correlations from interacting fibre-cavity polaritons, Nat. Mater. **18**, 213 (2019).

[21] A. Amo, D. Sanvitto, F. P. Laussy, D. Ballarini, E. d. Valle, M. D. Martin, A. Lemaître, J. Bloch, D. N. Krizhanovskii, M. S. Skolnick, C. Tejedor, and L. Viña, Collective fluid dynamics of a polariton condensate in a semiconductor microcavity, Nature (London) **457**, 291 (2009).

[22] A. Amo, J. Lefrère, S. Pigeon, C. Adrados, C. Ciuti, I. Carusotto, R. Houdré, E. Giacobino, and A. Bramati, Superfluidity of polaritons in semiconductor microcavities, Nat. Phys. **5**, 805 (2009).

[23] S. Kim, B. Zhang, Z. Wang, J. Fischer, S. Brodbeck, M. Kamp, C. Schneider, S. Höfling, and H. Deng, Coherent Polariton Laser, Phys. Rev. X **6**, 011026 (2016).

[24] J. D. Töpfer, I. Chatzopoulos, H. Sigurdsson, T. Cookson, Y. G. Rubo, and P. G. Lagoudakis, Engineering spatial coherence in lattices of polariton condensates, Optica **8**, 106 (2021).

[25] P. G. Savvidis, J. J. Baumberg, R. M. Stevenson, M. S. Skolnick, D. M. Whittaker, and J. S. Roberts, Angle-Resonant Stimulated Polariton Amplifier, Phys. Rev. Lett. **84**, 1547 (2000).

[26] M. Saba, C. Ciuti, J. Bloch, V. Thierry-Mieg, R. André, D. Le Si, S. Kundermann, A. Mura, G. Bongiovanni, J. Staehli, and B. Deveaud, High-temperature ultrafast polariton parametric amplification in semiconductor microcavities, Nature (London) **414**, 731 (2001).

[27] D. Ballarini, M. De Giorgi, E. Cancellieri, R. Houdré, E. Giacobino, R. Cingolani, G. Gigli, and D. Sanvitto, All-optical polariton transistor, Nat. Commun. **4**, 1778 (2013).

[28] C. Antón, T. C. H. Liew, G. Tosi, M. D. Martín, T. Gao, Z. Hatzopoulos, P. S. Eldridge, P. G. Savvidis, and L. Viña, Dynamics of a polariton condensate transistor switch, Appl. Phys. Lett. **101**, 261116 (2012).

[29] A. Zasedatelev, A. Baranikov, D. Urbonas, F. Scafirimuto, U. Scherf, T. Stöferle, R. Mahrt, and P. Lagoudakis, A room-temperature organic polariton transistor, Nat. Photonics **13**, 378 (2019).

[30] H. S. Nguyen, D. Vishnevsky, C. Sturm, D. Tanese, D. Solnyshkov, E. Galopin, A. Lemaître, I. Sagnes, A. Amo, G. Malpuech, and J. Bloch, Realization of a Double-Barrier Resonant Tunneling Diode for Cavity Polaritons, Phys. Rev. Lett. **110**, 236601 (2013).

[31] M. Klaas, J. Beierlein, E. Rozas, S. Klembt, H. Suchomel, T. Harder, K. Winkler, M. Emmerling, H. Flayac, M. Martin,

L. Vina, S. Höfling, and C. Schneider, Counter-directional polariton coupler, Appl. Phys. Lett. 114, 061102 (2019).

[32] F. Marsault, H. S. Nguyen, D. Tanese, A. Lemaître, E. Galopin, I. Sagnes, A. Amo, and J. Bloch, Realization of an all optical exciton-polariton router, Appl. Phys. Lett. 107, 201115 (2015).

[33] T. Gao, C. Antón, T. C. H. Liew, M. D. Martín, Z. Hatzopoulos, L. Viña, P. S. Eldridge, and P. G. Savvidis, Spin selective filtering of polariton condensate flow, Appl. Phys. Lett. 107, 011106 (2015).

[34] C. Sturm, D. Tanese, H. S. Nguyen, H. Flayac, E. Galopin, A. Lemaître, I. Sagnes, D. Solnyshkov, A. Amo, G. Malpuech, and J. Bloch, All-optical phase modulation in a cavity-polariton Mach-Zehnder interferometer, Nat. Commun. 5, 3278 (2014).

[35] S. Klembt, T. H. Harder, O. A. Egorov, K. Winkler, R. Ge, M. A. Bandres, M. Emmerling, L. Worschech, T. C. H. Liew, M. Segev, C. Schneider, and S. Höfling, Exciton-polariton topological insulator, Nature (London) 562, 552 (2018).

[36] A. Amo, T. Liew, C. Adrados, R. Houdré, E. Giacobino, and A. Kavokin, Exciton–polariton spin switches, Nat. Photonics 4, 361 (2010).

[37] T. Gao, P. S. Eldridge, T. C. H. Liew, S. I. Tsintzos, G. Stavrinidis, G. Deligeorgis, Z. Hatzopoulos, and P. G. Savvidis, Polariton condensate transistor switch, Phys. Rev. B 85, 235102 (2012).

[38] C. Antón, T. C. H. Liew, D. Sarkar, M. D. Martín, Z. Hatzopoulos, P. S. Eldridge, P. G. Savvidis, and L. Viña, Operation speed of polariton condensate switches gated by excitons, Phys. Rev. B 89, 235312 (2014).

[39] R. Cerna, Y. Léger, T. K. Paraïso, M. Wouters, F. Morier-Genoud, M. T. Portella-Oberli, and B. Deveaud, Ultrafast tristable spin memory of a coherent polariton gas, Nat. Commun. 4, 2008 (2013).

[40] R. Spano, J. Cuadra, C. Lingg, D. Sanvitto, M. D. Martin, P. R. Eastham, M. van der Poel, J. M. Hvam, and L. Viña, Build up of off-diagonal long-range order in microcavity exciton-polaritons across the parametric threshold, Opt. Express 21, 10792 (2013).

[41] G. Nardin, K. G. Lagoudakis, M. Wouters, M. Richard, A. Baas, R. André, L. S. Dang, B. Pietka, and B. Deveaud-Plédran, Dynamics of Long-Range Ordering in an Exciton-Polariton Condensate, Phys. Rev. Lett. 103, 256402 (2009).

[42] H. Ohadi, E. Kammann, T. C. H. Liew, K. G. Lagoudakis, A. V. Kavokin, and P. G. Lagoudakis, Spontaneous Symmetry Breaking in a Polariton and Photon Laser, Phys. Rev. Lett. 109, 016404 (2012).

[43] T. Horikiri, P. Schwendimann, A. Quattropani, S. Höfling, A. Forchel, and Y. Yamamoto, Higher order coherence of exciton-polariton condensates, Phys. Rev. B 81, 033307 (2010).

[44] M. Klaas, H. Flayac, M. Amthor, I. G. Savenko, S. Brodbeck, T. Ala-Nissila, S. Klembt, C. Schneider, and S. Höfling, Evolution of Temporal Coherence in Confined Exciton-Polariton Condensates, Phys. Rev. Lett. 120, 017401 (2018).

[45] J. Kasprzak, M. Richard, A. Baas, B. Deveaud, R. André, J.-P. Poizat, and L. S. Dang, Second-Order Time Correlations Within a Polariton Bose-Einstein Condensate in a CdTe Microcavity, Phys. Rev. Lett. 100, 067402 (2008).

[46] H. Ohadi, A. Dreismann, Y. G. Rubo, F. Pinsker, Y. del Valle-Inclan Redondo, S. I. Tsintzos, Z. Hatzopoulos, P. G. Savvidis, and J. J. Baumberg, Spontaneous Spin Bifurcations and Ferromagnetic Phase Transitions in a Spinor Exciton-Polariton Condensate, Phys. Rev. X 5, 031002 (2015).

[47] V. G. Sala, F. Marsault, M. Wouters, E. Galopin, I. Sagnes, A. Lemaître, J. Bloch, and A. Amo, Stochastic precession of the polarization in a polariton laser, Phys. Rev. B 93, 115313 (2016).

[48] A. Askitopoulos, L. Pickup, S. Alyatkin, A. Zasedatelev, K. G. Lagoudakis, W. Langbein, and P. G. Lagoudakis, Giant increase of temporal coherence in optically trapped polariton condensate, arXiv:1911.08981.

[49] K. Orfanakis, A. F. Tzortzakakis, D. Petrosyan, P. G. Savvidis, and H. Ohadi, Ultralong temporal coherence in optically trapped exciton-polariton condensates, Phys. Rev. B 103, 235313 (2021).

[50] P. Cilibrizzi, A. Askitopoulos, M. Silva, F. Bastiman, E. Clarke, J. M. Zajac, W. Langbein, and P. G. Lagoudakis, Polariton condensation in a strain-compensated planar microcavity with InGaAs quantum wells, Appl. Phys. Lett. 105, 191118 (2014).

[51] A. F. Adiyatullin, M. D. Anderson, P. V. Busi, H. Abbaspour, R. André, M. T. Portella-Oberli, and B. Deveaud, Temporally resolved second-order photon correlations of exciton-polariton Bose-Einstein condensate formation, Appl. Phys. Lett. 107, 221107 (2015).

[52] I. A. Shelykh, Y. G. Rubo, G. Malpuech, D. D. Solnyshkov, and A. Kavokin, Polarization and Propagation of Polariton Condensates, Phys. Rev. Lett. 97, 066402 (2006).

[53] J. J. Baumberg, A. V. Kavokin, S. Christopoulos, A. J. D. Grundy, R. Butté, G. Christmann, D. D. Solnyshkov, G. Malpuech, G. Baldassarri Höger von Högersthal, E. Feltin, J.-F. Carlin, and N. Grandjean, Spontaneous Polarization Buildup in a Room-Temperature Polariton Laser, Phys. Rev. Lett. 101, 136409 (2008).

[54] D. D. Solnyshkov, I. A. Shelykh, M. M. Glazov, G. Malpuech, T. Amand, P. Renucci, X. Marie, and A. V. Kavokin, Nonlinear effects in spin relaxation of cavity polaritons, Semiconductors 41, 1080 (2007).

[55] Ł. Kłopotowski, M. Martín, A. Amo, L. Viña, I. Shelykh, M. Glazov, G. Malpuech, A. Kavokin, and R. André, Optical anisotropy and pinning of the linear polarization of light in semiconductor microcavities, Solid State Commun. 139, 511 (2006).

[56] D. Read, T. C. H. Liew, Y. G. Rubo, and A. V. Kavokin, Stochastic polarization formation in exciton-polariton Bose-Einstein condensates, Phys. Rev. B 80, 195309 (2009).

[57] J. Kasprzak, R. André, L. S. Dang, I. A. Shelykh, A. V. Kavokin, Y. G. Rubo, K. V. Kavokin, and G. Malpuech, Build up and pinning of linear polarization in the Bose condensates of exciton polaritons, Phys. Rev. B 75, 045326 (2007).

[58] I. Gnusov, H. Sigurdsson, S. Baryshev, T. Ermatov, A. Askitopoulos, and P. G. Lagoudakis, Optical orientation, polarization pinning, and depolarization dynamics in optically confined polariton condensates, Phys. Rev. B 102, 125419 (2020).

[59] H. Sigurdsson, Hysteresis in linearly polarized nonresonantly driven exciton-polariton condensates, Phys. Rev. Research **2,** 023323 (2020).

[60] See Supplemental Material at http://link.aps.org/supplemental/10.1103/PhysRevLett.128.087402, which includes Refs. [61–68], for additional experimental data on polarization switching and pinning, details on dynamical mean field equations, and influence of residual laser polarization ellipticity on condensate.

[61] E. Del Valle, *Microcavity Quantum Electrodynamics* (VDM, Saarbrücken, 2010).

[62] Y. del Valle-Inclan Redondo, H. Ohadi, Y. G. Rubo, O. Beer, A. J. Ramsay, S. I. Tsintzos, Z. Hatzopoulos, P. G. Savvidis, and J. J. Baumberg, Stochastic spin flips in polariton condensates: Nonlinear tuning from GHz to sub-Hz, New J. Phys. **20,** 075008 (2018).

[63] M. Boozarjmehr, M. Steger, K. West, L. N. Pfeiffer, D. W. Snoke, A. G. Truscott, E. A. Ostrovskaya, and M. Pieczarka, Spatial distribution of an optically induced excitonic reservoir below exciton-polariton condensation threshold, arXiv:1912.07765.

[64] C. Ciuti, V. Savona, C. Piermarocchi, A. Quattropani, and P. Schwendimann, Role of the exchange of carriers in elastic exciton-exciton scattering in quantum wells, Phys. Rev. B **58,** 7926 (1998).

[65] M. Z. Maialle, E. A. de Andradae Silva, and L. J. Sham, Exciton spin dynamics in quantum wells, Phys. Rev. B **47,** 15776 (1993).

[66] L. Viña, Spin relaxation in low-dimensional systems, J. Phys. Condens. Matter **11,** 5929 (1999).

[67] M. Klaas, O. A. Egorov, T. C. H. Liew, A. Nalitov, V. Marković, H. Suchomel, T. H. Harder, S. Betzold, E. A. Ostrovskaya, A. Kavokin, S. Klembt, S. Höfling, and C. Schneider, Nonresonant spin selection methods and polarization control in exciton-polariton condensates, Phys. Rev. B **99,** 115303 (2019).

[68] L. Pickup, J. D. Töpfer, H. Sigurdsson, and P. G. Lagoudakis, Polariton spin jets through optical control, Phys. Rev. B **103,** 155302 (2021).

[69] M. Wouters and V. Savona, Stochastic classical field model for polariton condensates, Phys. Rev. B **79,** 165302 (2009).

[70] H. J. Carmichael, *Statistical Methods in Quantum Optics 1: Master Equations and Fokker-Planck Equations* (Springer Science and Business Media, Heidelberg, 2013).

[71] D. Witthaut, F. Trimborn, H. Hennig, G. Kordas, T. Geisel, and S. Wimberger, Beyond mean-field dynamics in open Bose-Hubbard chains, Phys. Rev. A **83,** 063608 (2011).

[72] C. Antón, S. Morina, T. Gao, P. S. Eldridge, T. C. H. Liew, M. D. Martín, Z. Hatzopoulos, P. G. Savvidis, I. A. Shelykh, and L. Viña, Optical control of spin textures in quasi-one-dimensional polariton condensates, Phys. Rev. B **91,** 075305 (2015).

[73] A. Askitopoulos, K. Kalinin, T. C. H. Liew, P. Cilibrizzi, Z. Hatzopoulos, P. G. Savvidis, N. G. Berloff, and P. G. Lagoudakis, Nonresonant optical control of a spinor polariton condensate, Phys. Rev. B **93,** 205307 (2016).

[74] M. D. Martín, G. Aichmayr, L. Viña, and R. André, Polarization Control of the Nonlinear Emission of Semiconductor Microcavities, Phys. Rev. Lett. **89,** 077402 (2002).

[75] I. Shelykh, G. Malpuech, K. V. Kavokin, A. V. Kavokin, and P. Bigenwald, Spin dynamics of interacting exciton polaritons in microcavities, Phys. Rev. B **70,** 115301 (2004).

[76] D. N. Krizhanovskii, D. Sanvitto, I. A. Shelykh, M. M. Glazov, G. Malpuech, D. D. Solnyshkov, A. Kavokin, S. Ceccarelli, M. S. Skolnick, and J. S. Roberts, Rotation of the plane of polarization of light in a semiconductor microcavity, Phys. Rev. B **73,** 073303 (2006).

[77] I. I. Ryzhov, V. O. Kozlov, N. S. Kuznetsov, I. Y. Chestnov, A. V. Kavokin, A. Tzimis, Z. Hatzopoulos, P. G. Savvidis, G. G. Kozlov, and V. S. Zapasskii, Spin noise signatures of the self-induced Larmor precession, Phys. Rev. Research **2,** 022064(R) (2020).

[78] A. Askitopoulos, H. Sigurdsson, I. Gnusov, S. Alyatkin, L. Pickup, N. A. Gippius, and P. G. Lagoudakis, Coherence revivals of a spinor polariton condensate from self-induced Larmor precession, arXiv:2006.01741.

[79] Y. del Valle-Inclan Redondo, H. Sigurdsson, H. Ohadi, I. A. Shelykh, Y. G. Rubo, Z. Hatzopoulos, P. G. Savvidis, and J. J. Baumberg, Observation of inversion, hysteresis, and collapse of spin in optically trapped polariton condensates, Phys. Rev. B **99,** 165311 (2019).

[80] 10.5258/SOTON/D2098.